Kinetics at the collapse transition of homopolymers and random copolymers

Yu. A. Kuznetsov, E. G. Timoshenko, and K. A. Dawson
Advanced Computational Research and Theory Groups, Centre for Soft Condensed Matter and Biomaterials, Department of Chemistry, University College Dublin, Dublin 4, Ireland

(Received 14 March 1995; accepted 12 June 1995)

We describe the results of Monte Carlo simulations for kinetics at the collapse transition of a homopolymer in a lattice model. We find the kinetic laws corresponding to the three kinetic stages of the process: $R_g^2(t)=R_g^2(0)-At^{7/11}$ at the early stage corresponding to formation and growth of locally collapsed clusters, the coarsening stage is characterized by growth of clusters according to the law $S \propto t^{1/2}$, where S is the average number of Kuhn units per cluster, and the final relaxation stage is described by the law $R_g^2(t)=R_g^2(\infty)+A_1^{(1)}e^{-t/\tau_1^{(1)}}$ with $\tau_1^{(1)} \propto N^2$. We also present preliminary results on the equilibrium properties and ''collapse'' transition of a random copolymer. The transition curve is determined as a function of hydrophobic bead concentration n_a. We discuss the different collapsed copolymer states as a function of the composition. At low hydrophilicity we believe the critical value of the interaction parameter is governed by the law $\chi_c(n_a) \propto n_a^{-2/3}$. In the kinetics we see unusual phenomena such as the appearance of a metastable long-lived states with few clusters and nontrivial loop structure. © *1995 American Institute of Physics.*

I. INTRODUCTION

Despite the fact that the equilibrium properties of polymer in dilute solutions have been quite extensively studied and well understood,[1–3] kinetic phenomena at the collapse transition are not so tractable by standard analytical methods and many aspects still remain unclear. There have been certain efforts to solve the problem numerically,[4] however the kinetic laws that govern this process have not yet been thoroughly elucidated. There are two approaches commonly used for computer simulations of polymer systems. One can proceed by straightforward numerical integration of, for example, the Langevin equation.[5] Alternatively, one can apply the method of Monte Carlo simulation.[6]

In this paper we present some results of Monte Carlo simulations of a lattice model of polymer dynamics and kinetics. Despite the simplicity and locality of the interactions, it is well known that this model yields the correct equilibrium exponents for an isolated homopolymer chain.[1–3,7] We believe that many of the kinetic exponents should also be correct. However, amongst its disadvantages we may mention that it is inconvenient to incorporate hydrodynamic interactions into lattice models, so for the moment most of our discussions are based on the neglect of hydrodynamics. The use of a lattice and the simple interaction Hamiltonian leads to a reduction of the calculational time compared to other models such as the continuous space Langevin simulations,[5] and it is possible to exhaustively study the problem with good statistical accuracy. In the present study we are able to obtain good averages for chains of lengths up to $N \sim 10^3$.

Similar lattice models are proving to be useful for other more complicated polymeric systems such as copolymers, and a three-component system of polymer, solvent and surfactant. We have given some preliminary results from our studies, but will later discuss more general issues. Here we focus on the equilibrium and kinetics of homopolymer and the quenched random copolymer ''collapse'' transition.

We note finally that the possibility of obtaining correct kinetic laws for the homopolymer collapse has long been understood in the community as a basic prerequisite to understanding biopolymer folding, as well as being of intrinsic scientific interest. Numerous people have contributed to the problem already, including de Gennes,[2] Ostrovsky, Rabin,[4,8] and colleagues of theirs. In this paper we aim to elucidate the situation for homopolymers, and open the discussion for copolymers.

II. METHOD OF THE SIMULATION

In this section we describe the model and some technical details of the Monte Carlo simulations of dynamics and kinetics at the collapse transition of polymer-water systems.

There are two obvious restrictions on the set of all possible updates or moves of the system. Namely, we must ensure polymer connectivity, and excluded volume. In a continuous-space model one requires a calculation of all forces to ensure that excluded volume is preserved, and there is an inner ''space'' loop in the Monte Carlo code. This can be avoided in a model with a finite-size discrete space, since a look-up table is used to manage this procedure. The dynamics can be performed by permutations of monomer and solvent beads on the lattice. We call such a permutation an elementary move.

Consider the model on a three-dimensional lattice with unit spacing. We restrict our model by making the following particular choices of elementary moves. The maximum distance between the nearest neighbors along the chain (NNC) is equal to $r_{\max}=\sqrt{3}$. Thus, for every bead the NNC are located in the nearest lattice sites along the vertices of the lattice, or on second or third lattice neighbors. This condition provides for connectivity of the chain. Furthermore, excluded volume is incorporated by ensuring that only NNC are permitted in the nearest neighbor lattice sites, i.e., the

minimum distance between beads is $r_{\min}=1$ for NNC beads (NNC cannot overlap), and $r_{\min}=\sqrt{2}$ otherwise.

The model discussed above is described by the Hamiltonian,

$$H=\frac{1}{2}\sum_{i\neq j} w(r_{ij})\mathscr{J}_{s_i s_j}, \tag{1}$$

where i, j enumerate lattice sites; s_i labels the state of site i, $\mathscr{J}_{s_i s_j}$ is a 2×2 symmetric matrix of monomer–monomer $\mathscr{J}_{mm}$, monomer–solvent $\mathscr{J}_{ms}$, and solvent–solvent $\mathscr{J}_{ss}$ interaction constants, respectively; $r_{ij}=|\mathbf{r}_i-\mathbf{r}_j|$ and $w(r_{ij})$ is some function giving the form of the potential interaction with the property $w(1)=1$. In principle Hamiltonian (1) implies that each lattice site interacts with all others. There are no simplifications for a model with long-range interactions, but for short-range interactions we write $w(r)=0$, for $r>R_{\max}$, where $R_{\max}$ is some range of interaction. In our model we chose $w(\sqrt{2})=1$, $w(\sqrt{3})=0.7$, $w(2)=1/2$ and $w(r)=0$ for $r>2$. Thus, the range of interaction includes the nearest and second-nearest neighbors.

We have used the Metropolis algorithm[6] for calculation of the transition probability in a system at temperature T. In particular, the probability of an elementary move, where a monomer escapes from interaction volume of another one, can be expressed in the form,

$$\eta=\exp(-w(r)\chi), \tag{2}$$

where r is the initial distance between monomers and χ is interaction parameter defined as

$$\chi\equiv\frac{2\mathscr{J}_{ms}-\mathscr{J}_{mm}-\mathscr{J}_{ss}}{k_B T}. \tag{3}$$

From physical considerations (see, e.g., Ref. 2) it follows that $\chi\geqslant 0$.

We may note that there is only one parameter χ that determines the thermodynamical properties of the system for a given degree of polymerization N, and lattice size L. We consider only lattice sizes larger than the configurations explored by the simulation, so there is no need to apply special boundary conditions.[9] Finally, we call the sequence of attempts to move each polymer bead once, a Monte Carlo sweep (MCS). The latter is assumed to play the role of the discrete time unit.

It is also necessary for us to introduce the notion of a cluster since this will be useful in the study of kinetics at the collapse transition of polymers. We say that a set of polymer beads form a cluster if the maximal distance between them does not exceed some value $l_{\max}$. We also apply the constraint that the number of particles in the cluster must be more than $n_{\min}$. We have used the scheme in which $l_{\max}^2=4$, i.e., $l_{\max}$ is equal to interaction range, and $n_{\min}=10$. However, the essential results, as we show later, are not affected by the details of such choices. We use two observables connected with above definition, namely the average number of clusters per chain $\langle n\rangle$, and average number of monomers in clusters S.

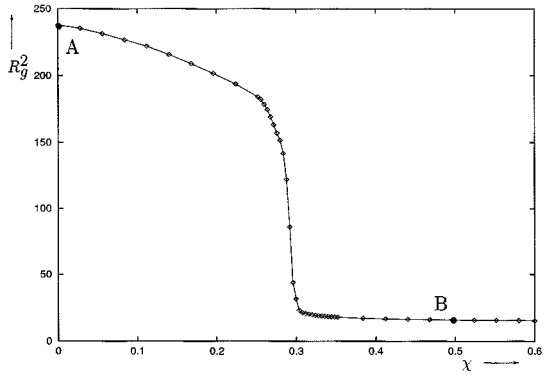

FIG. 1. Plot of the equilibrium radius of gyration squared versus the interaction parameter χ for homopolymer with degree of polymerization $N=256$.

III. EQUILIBRIUM PROPERTIES OF A HOMOPOLYMER

In this section we intend to comment that the equilibrium properties of the homopolymer model described above are in good agreement with well-known results from other approaches and previous studies.[1–3] In addition, however, we shall introduce and calculate various correlation functions that are not normally discussed. These correlation functions will be useful as we present our nonequilibrium studies, and in any case they are the main quantities that are calculated in recent theoretical discussions.[10,11] To begin with we have studied various equilibrium observables to check the simulation, and to determine the locations of collapse transitions.

In Figs. 1 and 2 we illustrate the mean-square radius of gyration, and heat capacity of the system as a function of the parameter χ:

$$R_g^2\equiv\frac{1}{N^2}\sum_{n<m}\langle(\mathbf{r}_n-\mathbf{r}_m)^2\rangle, \tag{4}$$

$$C_V\equiv(\langle E^2\rangle-\langle E\rangle^2)/k_B T^2. \tag{5}$$

In (4) the indexes n, m run over the polymer chain. One can see from Eqs. (2) and (3) that the energies of all microstates of the system are equal at the point $\chi=0$, and consequently $C_V=0$. At the point $\chi_c\approx 0.295$, where the heat capacity C_V reaches its maximal value, the system undergoes

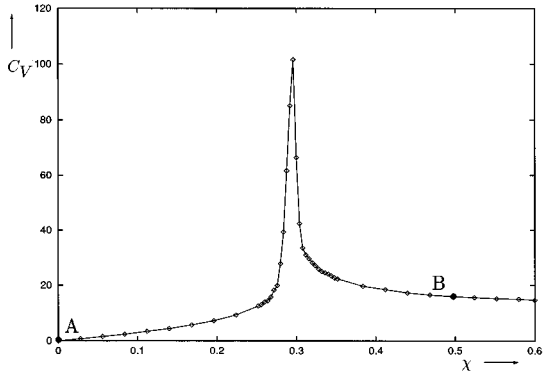

FIG. 2. Plot of the equilibrium heat capacity versus the interaction parameter χ for degree of polymerization $N=256$.

TABLE I. Values of the radius of gyration square for the good ($R^2_{g,F}$) and poor ($R^2_{g,C}$) solvent equilibrium states and values of interaction parameter χ_c at the θ point for a homopolymer of different degrees of polymerization N (Ref. 13).

N	32	64	80	128	160	180	256	384	512
$R^2_{g,F}$	18.3	49	64	117	150	175	237	416	556
$R^2_{g,C}$	3.76	5.88	6.9	9.52	11.1	12.0	15.2		
χ_c	0.42	0.36	0.33	0.31	0.30	0.30	0.295		

a precipitous collapse transition. As can be seen from the Table I, the values of χ_c do not depend essentially on the degree of polymerization N for $N>150$, having risen from a somewhat bigger value for shorter chain length.

Evidently the range $\chi<\chi_c$ corresponds to good solvent conditions and there the Flory coil is preferred. Across the collapse transition R_g decreases strongly coming, finally, to the fully collapsed single-globule configuration. The values of the radius of gyration square R_g^2 for both the Flory coil and the collapsed state as a function of chain length are given in Table I. Using the definition of the swelling exponent,

$$R_g = bN^{\nu}, \tag{6}$$

we find $b=0.6\pm0.05$, and $\nu=0.59\pm0.03$ for the Flory state and $\nu=0.336\pm0.004$ for the collapsed state, in agreement with the best estimates from all other methods, including the ''mean-field''[12] values of $\nu=3/5$ and $\nu=1/3$, respectively. The value of the parameter b in (6) is not universal and depends on the model.

The principle observables of the system of current interest to us are the correlation functions $\langle \mathbf{r}_n(t)\mathbf{r}_{n'}(t')\rangle$ with equal and different times. However in practice it is more convenient to work with the Fourier transformed variables defined for open polymers by the transformations:[14]

$$\mathbf{r}_q = \sum_{n=0}^{N-1} \cos\left(\frac{\pi q(n+1/2)}{N}\right)\mathbf{r}_n,$$
$$\mathbf{r}_n = \frac{2-\delta_{q0}}{N}\sum_{q=0}^{N-1} \cos\left(\frac{\pi q(n+1/2)}{N}\right)\mathbf{r}_q. \tag{7}$$

This transformation does not, of course, simplify the Hamiltonian (1) but it does allow us to present the radius of gyration in the diagonal form:

$$R_g^2 = \sum_{q=1}^{N-1} F_q, \tag{8}$$

$$F_q(t) = \langle \mathbf{r}_q^2(t)\rangle, \tag{9}$$

as well as providing direct comparison to theoretical calculations.[15]

Note that the formulas above are exact, though when excluded volume is accounted for, the Fourier modes are not simply those of the Rouse or Zimm models since, strictly speaking, $\langle \mathbf{r}_q\mathbf{r}_{q'}\rangle \neq F_q\delta_{qq'}$. However, only the diagonal elements contribute to the radius of gyration (8). It has been shown in Refs. 16, 10 that at equilibrium one has the scaling,

$$F_q^{(e)} \propto q^{-2\beta}, \quad \beta = \nu + 1/2, \tag{10}$$

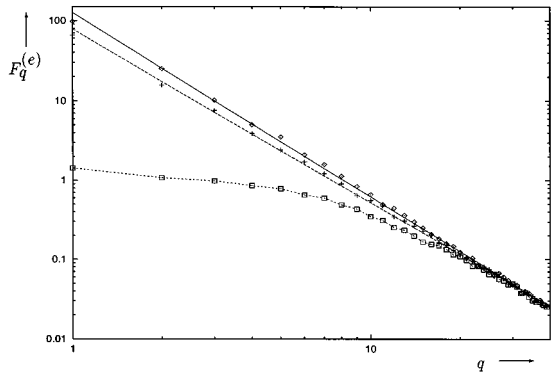

FIG. 3. Logarithmic plot of the internal modes $F_q^{(e)}$ (at equilibrium) versus q in the region $q=1,...,40$ for the degree of polymerization $N=160$ for different values of the interaction parameter χ: $\chi=0$, $\chi=0.2$ and $\chi=1.0$ (from top to bottom). Straight lines correspond to power fit of the data at $\chi=0$ and $\chi=0.2$.

where ν is the swelling exponent, and q is not too large.

In Fig. 3 we exhibit the dependence of $F_q^{(e)}$ versus q for the chain index q running from 1 to 40. The solid line yields the power law fit to the points of $F_q^{(e)}$ at $\chi=0$ and its slope corresponds to the exponent $\beta(0.0)=1.15$. The long-dashed line corresponds to the point $\chi=0.2$ and yields the exponent $\beta(0.2)=1.088$. The other dashed line represents $F_q^{(e)}$ for $\chi=1.0$ at which point the chain is in the collapsed state. In this case the first seven internal modes do not satisfy a power law. A power fit in the middle region gives $\beta(1.0)=0.85-0.90$ (the theoretical value is 5/6). As might be expected, therefore, on the lattice the collapsed state value of the exponent ν is reliably determined only from the scaling of the radius of gyration [see the results after Eq. (6)], whilst for extended states both criteria are satisfactory with $F_q^{(e)}$ and R_g^2 giving the upper and lower bound on its value respectively. These functions, $F_q^{(e)}$, are very useful in our studies of kinetics since they permit us to make relation to the theory, and thereby to such concepts as spinodal decomposition.[11]

IV. KINETICS AT THE COLLAPSE TRANSITION OF A HOMOPOLYMER

The purpose of this section is to present the main kinetic laws that govern the collapse transition of a homopolymer. Our results confirm the collapse mechanism proposed in previous works[5,11,15] and some conclusions are in agreement with scaling results from various works.[17,4] The present paper represents an effort to solve the problem from the point of view of the lattice model with no *a priori* restrictions, and with sufficient precision to be able to establish the various exponents with certainty.[18] Thus, the simplicity and reduction of calculation time required by a lattice model compared to the continuous space Langevin simulation[5] permits us to resolve many of the open questions.

We can say that our simulation allows us to argue for at least four different kinetic stages following an abrupt quench into collapse globule region of the phase diagram. Some theoretical considerations support this thinking. We study the first three of these, since the final late stage equilibration of

the compact collapsed state is improperly described by a lattice model. Thus, the system is first equilibrated in the Flory coil state. We then increase the interaction parameter χ in Eq. (3) by some value $\Delta\chi$ and observe the evolution of the system. Averages are understood in the conventional nonequilibrium statistical mechanical sense of averaging over initial conditions. The value $\Delta\chi$ that we consider may be characterized as a sufficiently small quench to maintain mobility of the chain. However we emphasize that it carries us sufficiently beyond the θ-point for the heat-capacity to have fallen to normal values. In this sense, and according to the normal expectations in nonequilibrium statistical mechanics, we can say that we have passed completely through the transition. The initial and final values of the interaction parameter χ are equal to $\chi_i = 0$ and $\chi_f = 1/2$ and are denoted by large dots labeled A and B respectively in Figs. 1 and 2.

(1) The earliest kinetic stage is characterized by rapid formation of numerous small collapsed globules. This process is essentially local and its duration is quite independent of the degree of polymerization. An example of a particular polymer configuration during this stage is drawn in Fig. 4. Figure 4(a) corresponds to an equilibrium polymer configuration in the Flory coil state. One can see numerous small and comparatively low-density accumulations of monomers present in that state and after the quench these become sites for the formation of locally collapsed globules. This situation is drawn in Fig. 4(b) and the configuration there corresponds, approximately, to the end of the first kinetic stage. It is worth noting that the matter of cluster definition in our work is no more problematic than in, for example, work in diffusion limited aggregation. It is, of course, not unique, but within reasonable bounds of definition we find the same picture, and laws pertain.

The first kinetic stage corresponds to rapid initial growth of the average number of clusters $\langle n \rangle$ and average number of monomers in a cluster S, which is consistent with mechanism of globule formation. The typical situation for the average number of clusters is shown at the top of Fig. 5 (lines labeled $N = 768$ and $N = 768^*$). Note that these values of $\langle n \rangle$, obtained using two different cluster definitions, are quantitatively different during approximately the first 500 MCS. Nevertheless, further evolution shows convergence of the curves. It may be observed from Fig. 4(b), that after the earliest stage of kinetics, the polymer configuration contains several quite distinguishable clusters. We find that the qualitative behavior of the cluster observables S and $\langle n \rangle$ during subsequent kinetic stages is independent of the cluster definition scheme, and the exponents are unchanged.

Now, the mean-square radius of gyration decreases very sharply during the earliest kinetic stage and can be approximated by the formula,

$$R_g^2(t) = R_0^2 - At^{\alpha}, \quad \alpha = 0.66 \pm 0.03, \tag{11}$$

for polymers of chain lengths about 100–1000. Some particular values of the exponent α for different degrees of polymerization are given in Table II. One would naturally expect a linear decrease at the earliest times, but the data do not support this, nor does the theory presented in Refs. 11 and 19.

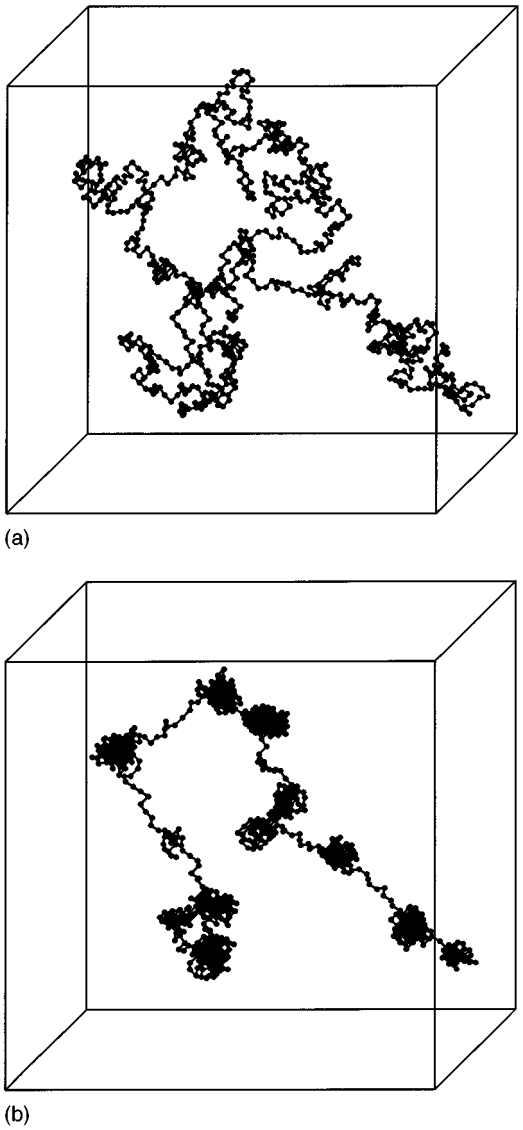

FIG. 4. The kinetic evolution of a particular polymer configuration during the first kinetic stage. The degree of polymerization and the linear lattice size equal to $N = 768$ and $L = 128$ respectively. The size of the frame in these and subsequent figures is two times smaller than the real size of the lattice. The upper picture (a) shows the polymer in the equilibrium extended Flory coil state, and the lower picture (b) represent the same configuration after 1000 MCS, thus corresponding, approximately, to the end of the earliest kinetic stage.

Thus, during this early stage, the main change of the radius of gyration arises from the large-q internal modes in (9), even though their amplitude is a decreasing function of q. The small-q modes hardly change at early time. We have elsewhere interpreted these effects more precisely in terms of a type of spinodal decomposition mechanism in the internal metric of the chain. In this description[11] the high-q modes decrease exponentially at small time. In any case, we can see that the decrease in amplitude of high-q modes corresponds to shrinking of the polymer at small distances, i.e., formation of small dense clusters.

Furthermore, the exponent α in the formula (11) may be interpreted in the framework of the Gaussian self-consistent approach. As indicated in an earlier paper[11] the first kinetic

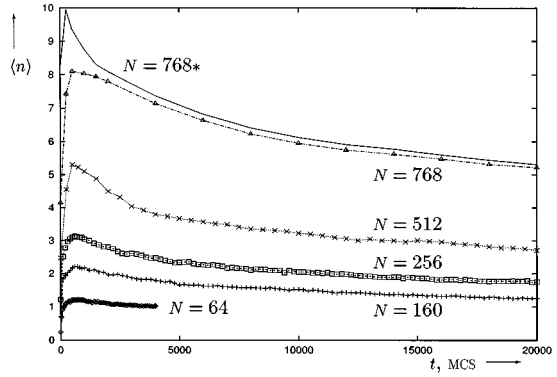

FIG. 5. The average number of clusters per polymer chain $\langle n \rangle$ versus time in MCS units for different degrees of polymerization (from bottom to top): 64, 160, 256, 512, 768. The solid line labeled as 768* corresponds to the values of $\langle n \rangle$ for polymer with the degree of polymerization $N=768$, obtained using other cluster definition parameters (see Chap. 2): $l^2_{\max}=4$, $n_{\min}=7$.

stage was investigated by linearizing the nonequilibrium equations of motion for the internal modes $F_q(t)$ (see formula (34) in Ref. 11). The deviation from the equilibrium value may be sought in the form

$$\Delta F_q = \mathscr{A}_q(1-e^{-\lambda_q t}) \simeq B_q t + C_q \frac{t^2}{2} + \cdots, \quad \lambda_q \simeq -C_q/B_q . \tag{12}$$

The few first internal modes with $q<q_c$ are unstable, i. e. $\lambda_q<0$ for small times when the linear representation (12) is valid. Their contribution to the radius of gyration becomes significant at that stage, but for very early times, say $t \leqslant 1/|\lambda_{\max}|$, where $\lambda_{\max}$ is the maximal unstable value, the main change of R_g^2 is due to the first Taylor term in (12). The functions B_q and λ_q scale for sufficiently large q as:[20]

$$B_q \propto \underline{q}^{3\nu-2}, \quad \lambda_q \propto \underline{q}^{2\nu+1}, \tag{13}$$

where $\underline{q}=q/\pi N$ and $\nu=3/5$ is the Flory exponent. Therefore R_g^2 mainly changes due to changes in the large q (stable) modes. Thus ignoring the contributions of unstable modes $q<q_c$, the deviation of the radius of gyration square $\Delta R_g^2(t)$ may be written as

$$\Delta R_g^2(t) = \sum_{q>q_c} \mathscr{A}_q(1-e^{-\lambda_q t}) \simeq \int_{\underline{q}_c}^{\infty} d\underline{q}\, \mathscr{A}_{\underline{q}}(1-e^{-\lambda_{\underline{q}} t})$$

and using the scalings (13) one finds,

$$\Delta R_g^2(t) \propto t^{(2-\nu)/(2\nu+1)} = t^{7/11}, \quad t<1/|\lambda_{\max}|, \tag{14}$$

which agrees with the result of simulations (11). With this argument we are able to identify the crossover time for the first stage to be determined by $1/|\lambda_{\max}|$, but we note that no simulation evidence exists for this as yet, and we base this assertion only on theoretical arguments. On the other hand, there is compelling evidence for Eq. (11) from theory and simulation. Also, simulations not discussed here clearly show the presence of unstable modes, and theory is quite clear on this matter too.

TABLE II. Numerical values of the exponent α in (11) obtained from the fit of change of the radius of gyration squared during the first 100 MCS for homopolymers of different degrees of polymerization N. Each value was obtained from many hundreds of copies of the system, and stability of the results to improve the sample was checked.

N	96	160	256	512	768	1024
α	0.65	0.64	0.69	0.66	0.67	0.66

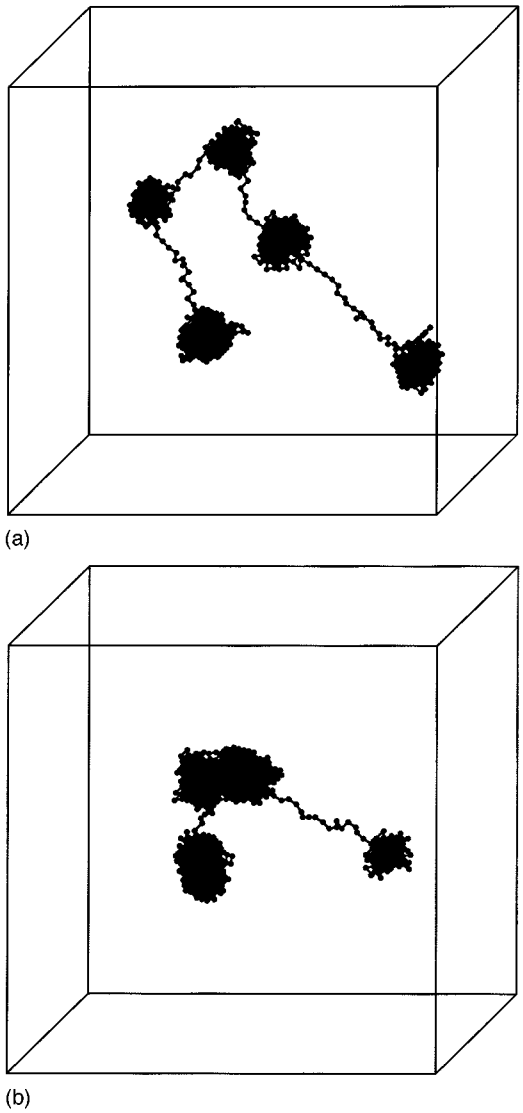

FIG. 6. Evolution of a particular polymer configuration with degree of polymerization $N=768$ on the lattice $L=128$ during the coarsening kinetic stage. Pictures (a) and (b) correspond, respectively, to times 40 000 and 160 000 MCS after the quench.

(2) The second or ''coarsening'' stage may be characterized by the law of ''blob'' growth. In Fig. 6 we present a configuration from this stage of kinetics where the initial configuration was the Flory coil state of Fig. 4(a). In the simulations it is clear that growth of blobs proceeds mainly by unification with smaller ones. Polymer segments linking different globules are quite tight and accretion of monomer units from such segments by the neighboring globules gives a much less significant contribution. The main growth mechanism at the quenches we have studied is not, in fact, end dominated,[4] a process that might be relevant at deep

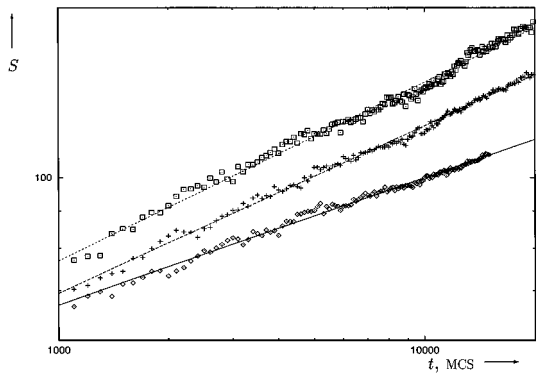

FIG. 7. Logarithmic plot of the average cluster size S versus t during the coarsening kinetic stage for different degrees of polymerization (from bottom to top): 128, 160, and 256.

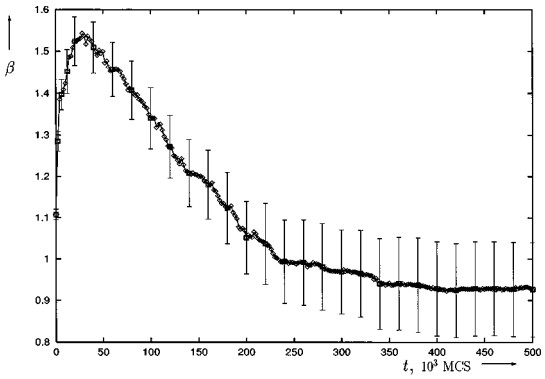

FIG. 8. Effective power exponent $\beta(t)$ from internal modes $F_q(t)$ versus time t ($q=2,...,20$) for degree of polymerization $N=768$. Error bars gives the approximation of the quality of power fit (10).

quenches. Instead, the surface of the bloblike clusters is quite mobile and permits shape fluctuations that allows the capture of comparatively close globules. Note that this does not lead to completely compacted clusters at this stage, and a fair degree of mobility of the chains persists even inside the collapsed globules.

At this stage the cluster growth law can be described by the power law,

$$S_N = A_N t^{Z_N}. \tag{15}$$

This function is exhibited in Fig. 7 for polymers of different chain lengths using a logarithmic scale. The subscript N in (15) denotes a dependence of these parameters on the degree of polymerization for finite length polymers. Numerical values of $\log A_N$, Z_N obtained from the simulations of different polymers and their total collapse times $\tau_S(N)$, defined as,

$$\tau_S(N) \equiv (N/A_N)^{1/Z_N} \tag{16}$$

are presented in Table III. The formula (16) can be obtained from the cluster growing law (15) by setting $S=N$ in the latter. The exponent Z_N tends to 1/2 for sufficiently large polymers. The average number of clusters $\langle n \rangle$ may be approximated as

$$\langle n \rangle \approx N/S, \tag{17}$$

and hence it decreases in time as a power law.

We note that Eq. (15) for cluster growth shares much with the law of Lifshitz and Slyozov[21] for liquid droplet growth. The difference here is that the material being absorbed to the droplets is topologically constained, and there is a tension in the polymer that tends to prevent compaction onto the condensed clusters. The dominant effect at this stage seems to be that the coil behaves as a nearly ideal chain of globules. The elastic response of this chain produces an effective growth exponent $Z_\infty = 1/2$.

TABLE III. Values of parameters (natural) $\log A_N$ and Z_N of the cluster growth law in (15) and the total and characteristic collapse times τ_s and $\tau_1^{(1)}$ for polymers of different degree of polymerization N.

N	64	128	160	256	512	768
$\log A_N$	2.90	3.03	2.65	2.63	0.628	0.278
Z_N	0.151	0.174	0.223	0.247	0.422	0.445
$\tau_S(N)$, 10^3 MCS	4.18	35.3	52.4	132	594	1632
$\tau^{(1)}$, 10^3 MCS	1.93	9.35	15.6	41.3	151.5	476.2
$\tau_S(N)/\tau_1^{(1)}(N)$	2.17	3.77	3.36	3.20	3.92	3.43

The dependence of the internal mode functions $F_q(t)$ on q is not quite a power law in q. Nevertheless, the effective power $\beta(t)$ can be evaluated for small values of q. This dependence for the first and second kinetics stages is exhibited in Fig. 8. The exponent, $\beta(t)$, changes rapidly during the earliest kinetic stage and continues to grow during coarsening, reaching its maximum value close to the value $\beta_{max}=3/2$, corresponding to a rigid rod exponent. This is in accordance with observations of typical configurations. Thus, for example the regime of Fig. 4(b) corresponds to a growing effective exponent β until, roughly, Fig. 6(a). Beyond this stage we have a long slow decrease of the effective exponent β corresponding to the regime between Figs. 6(a) and 6(b). The quality of a power fit of the nonequilibrium internal modes $F_q(t)$ on q is shown in Fig. 8 by error bars. The latter approximate the correspondence of the internal modes to the power law (10).

In agreement with theory,[11] our simulations indicate that the dependence of the first few internal modes on time can be very well approximated by a two-exponential relaxation law,

$$F_q(t) = b_q + A_q^{(1)} \exp(-t/\tau_q^{(1)}) + A_q^{(2)} \exp(-t/\tau_q^{(2)}), \quad \tau_q^{(1)} > \tau_q^{(2)}. \tag{18}$$

Numerical values of the amplitudes $A_q^{(1,2)}$ and the relaxation rates $\tau_q^{(1,2)}$ decrease with q. We may also note that the high-q internal modes change relatively little at this stage. Thus, only the first few internal modes give the main contribution to the evolution of the radius of gyration square R_g^2 at the coarsening kinetic stage [see Eq. (8)]. In Fig. 9 the evolution of $R_g^2(t)$ for different polymers lengths is shown. We note that the final value of R_g^2 estimated from this data appears to be close to the one obtained from the equilibrium collapse state. The longest-time exponent $\tau_1^{(1)}$ in (18) may be considered as a characteristic collapse time at this stage, though there are undoubtedly even longer time scales connected to compaction. However, these processes have little effect on changes of the radius of gyration and therefore are not re-

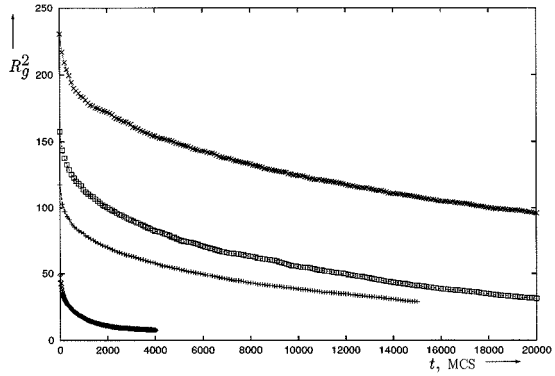

FIG. 9. The radius of gyration squared $R_g^2(t)$ versus time t for different degrees of polymerization (from bottom to top): 64, 128, 160, 256.

flected, we believe, in the total collapse time τ_S. Numerical values of $\tau_1^{(1)}$ for polymers of different chain length are given in Table III. Comparison of $\tau_1^{(1)}$ with the collapse time obtained from (15) is also given in Table III. Both the total collapse time τ_S and characteristic collapse time $\tau_1^{(1)}$ can well be approximated as the square of the degree of polymerization N (Ref. 22)

$$\tau_1^{(1)} \propto N^{2.03\pm0.06}, \quad \tau_S \propto N^{2.08\pm0.13}. \tag{19}$$

This scaling may naively be viewed as a Rouse relaxation and we note that it agrees with the exponent cited by de Gennes in the absence of hydrodynamics.[17] However, as noted above, we emphasize once more that the origin of this exponent lies in the coarsening mechanism discussed above. This is a local accretion mechanism that is hardly comparable to any Rouse processes. However, the latter does impose a bound on the collapse relaxation time, providing topological barriers to collapse are negligible. Rather, we interpret the exponent Z, as originating from growth of globules against the elasticity of an ideal chain of locally collapsed globules for which the Flory exponent is close to $\nu = 1/2$. By elementary arguments it would be easy to obtain the results

$$Z_\infty = \frac{1}{2\nu + 1}, \tag{20}$$

where ν is the effective exponent.

(3) The next relaxation stage can be characterized as a slow approach to the final collapsed state. Figure 10 illustrates this stage for the particular polymer configuration that was previously shown in Figs. 4 and 6. The processes that play a significant role during this stage are compactification of internal structure of the collapsed globule and optimization of its surface, which tends to be a sphere. Note that some configurations of the ensemble do not collapse to a single globule during the coarsening stage, especially for very long polymer chains. The complete unification of these clusters occurs only in the final stage. The ensemble average squared radius of gyration decays with an exponential law with the most long-lived relaxation time $\tau_1^{(1)}$.

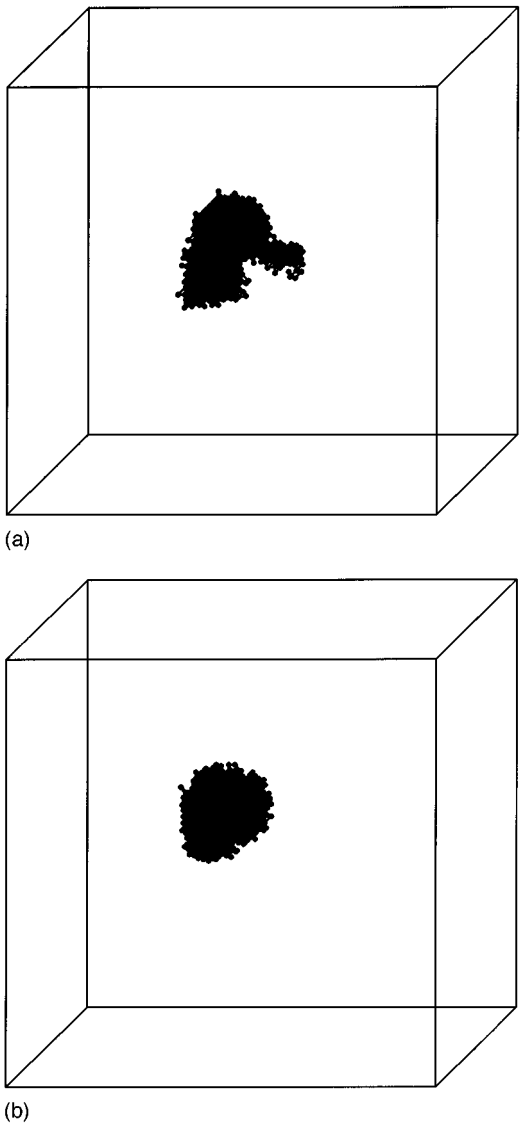

FIG. 10. Evolution of a particular polymer configuration with degree of polymerization $N = 768$ on the lattice $L = 128$ during the final kinetic stage: (a) and (b) pictures correspond to times 450 000 and 500 000 MCS after the quench.

(4) Final compactifications and rearrangements of the globule represent the last stage, but are not discussed in this paper. These late stages are issues that are better treated by ideas discussed in other papers.[23]

V. RANDOM COPOLYMERS: EQUILIBRIUM AND KINETICS

Copolymer systems, in which different polymer beads have different interaction properties with solvent, are currently of considerable interest to the scientific community both for intrinsic scientific interest, but also as models of biopolymers.[24,25] To be specific, the sort of systems that we have in mind are those where one monomer is always hydrophilic, and the other has amphiphilic properties that can cause it to pass from mostly hydrophilic to hydrophobic properties.[26] Such systems as copolymers of acrylamide and N-isopropylacrylamide would be explicit examples of the

systems we have in mind. Even the equilibrium properties of these polymers at infinite dilution are rather poorly understood at the minute, though some researches are beginning to be published in the theoretical and experimental literature.[27–31] In this chapter we present preliminary results of our study of equilibrium, dynamics and kinetics near the collapselike transition of random copolymers.

We consider a model of a random copolymer consisting of only two different monomer types randomly distributed along the chain. The total number of each monomer type is held fixed for every configuration in the ensemble. The chain structure does not change under time evolution. Formally, a copolymer–solvent interaction may be described in the same fashion as the homopolymer one, namely by the Hamiltonian (1), where the matrix indexes s_i takes three different values, solvent s and monomer types denoted as a and b. Thus, in contrast to homopolymers, where the only interaction parameter is χ, copolymers can be described by three parameters:

$$\chi_{aa}=\frac{2\mathscr{J}_{sa}-\mathscr{J}_{aa}-\mathscr{J}_{ss}}{k_BT},$$

$$\chi_{bb}=\frac{2\mathscr{J}_{sb}-\mathscr{J}_{bb}-\mathscr{J}_{ss}}{k_BT}, \tag{21}$$

$$\chi_{ab}=\frac{\mathscr{J}_{sa}+\mathscr{J}_{sb}-\mathscr{J}_{ab}-\mathscr{J}_{ss}}{k_BT}.$$

By analogy to the homopolymer case [see Eqs. (2) and (3)], these correspond to the change in interaction when a given monomer–monomer arrangement is changed from interacting to noninteracting after an elementary move. Thus, the probability of such a move is equal to: $\eta=\exp(-w(r)\chi)$, where χ is given by (21). We shall consider only a special cut of parameter space with the condition, $\mathscr{J}_{aa}+\mathscr{J}_{bb}=2\mathscr{J}_{ab}$. We can therefore reduce the number of parameters to two via the relation, $\chi_{ab}=(\chi_{aa}+\chi_{bb})/2$. We further restrict our model by assuming that the b–monomers are hydrophilic, $\chi_{bb}=0$. Thus we have two parameters describing a copolymer–solvent system, the hydrophobicity parameter χ_{aa} of a-monomers and their relative concentration $n_a=N_a/N$. Simulation of these random copolymers is carried out in a manner analogous to the simulation of homopolymers. The only difference is that one starts from particular a- and b-monomer sequences, selected from a uniform random distribution on the interval [0, 1], and then we finally average the results over all such chain distributions. Our procedure corresponds to the quenched disorder case, because the location of both hydrophilic and hydrophobic monomers is fixed along the chain.[28] We note that other related models have been discussed recently in the literature.[30,25] In particular we would like to point to the work in Ref. 32 where a sort of random ''charge'' model has been studied and where some phenomena comparable to those we observed such as glass transitions and microphase separation have appeared. We attempt to study a different Hamiltonian to theirs, and as we shall see the manifestation of these concepts is somewhat different.

The phase diagram, exhibited in Fig. 11, is obtained from simulations of the copolymer with degree of polymerization $N=180$. The curve separating two different phases corresponds to the value of critical interaction parameter χ_c versus concentration n_a. The values of χ_c are determined from the peaks in the heat capacity. At this point we emphasize that the lower part of the phase diagram is certainly Flory phase, but the upper part, collectively labeled ''collapsed,'' corresponds in fact to a variety of states, extending from simple collapsed for pure homopolymer, to only partially collapsed in the region $n_a \lesssim 1/5$. Thus, the absolute radius has decreased throughout the phase diagram, but the Flory exponent is roughly 1/3 only for $n_a \gtrsim 1/5$. We note that in the range of comparatively large hydrophobic monomer concentration, say $n_a \gtrsim 1/10$, the critical parameter may be well approximated by the formula,

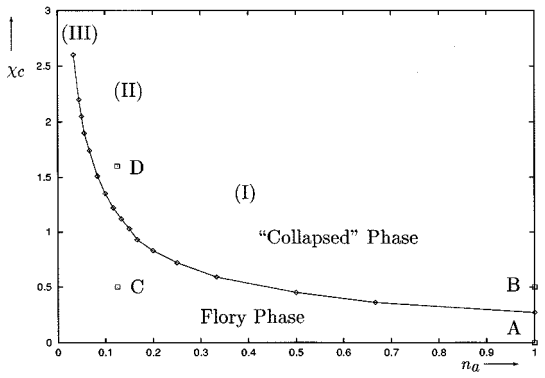

FIG. 11. Phase diagram for random copolymer with the degree of polymerization $N=180$. The solid line corresponds to the dependence of the critical point value χ_c of the interaction parameter χ_{aa} on the hydrophobic bead concentration n_a. The points A and B correspond, approximately, to the quench made in the homopolymer study (see also Figs. 1 and 2) of Figs. 4–10. The points C and D correspond, approximately to the quench made in the copolymer study to be presented in the Fig. 13. Regions of the diagram are labeled by the numbers, (I), (II) and (III). Region (III) corresponds to a chain of small micelles, probably a renormalized Flory coil. Region (II) may be a crossover between these, but it corresponds to a few quite large micellar objects.

$$\chi_c=\chi_c^{(h)}n_a^{-2/3}, \tag{22}$$

where $\chi_c^{(h)}$ is the critical interaction parameter for homopolymers.

Now, as noted above, the lower region of the phase diagram corresponds to the Flory coil phase, and the upper to what we call the ''collapsed'' state. We now note also that the typical copolymer configurations of the ''collapsed'' phase are quite different from the simple homopolymer globule. In general the ''collapsed'' phase of the copolymers consists of micellelike collapsed hydrophobic cores surrounded by the hydrophilic b-monomer shell[28] as presented in Fig. 12(b). For comparatively large hydrophobic concentrations, $n_a \gtrsim 1/5$, the configuration tends to be a single micellar state and the hydrophilic shell is quite dense. This corresponds to region (I) in the phase diagram in Fig. 11. At the smallest hydrophobic concentrations, $n_a \lesssim 1/10$, equilibrium configurations are composed of a chain of ''micelles,'' where the hydrophobic material is gathered into the cores, and the exteriors of the micelles are composed of hydrophilic monomers. This corresponds to region (III) in the phase diagram in Fig. 11. In between these two regimes, in the area

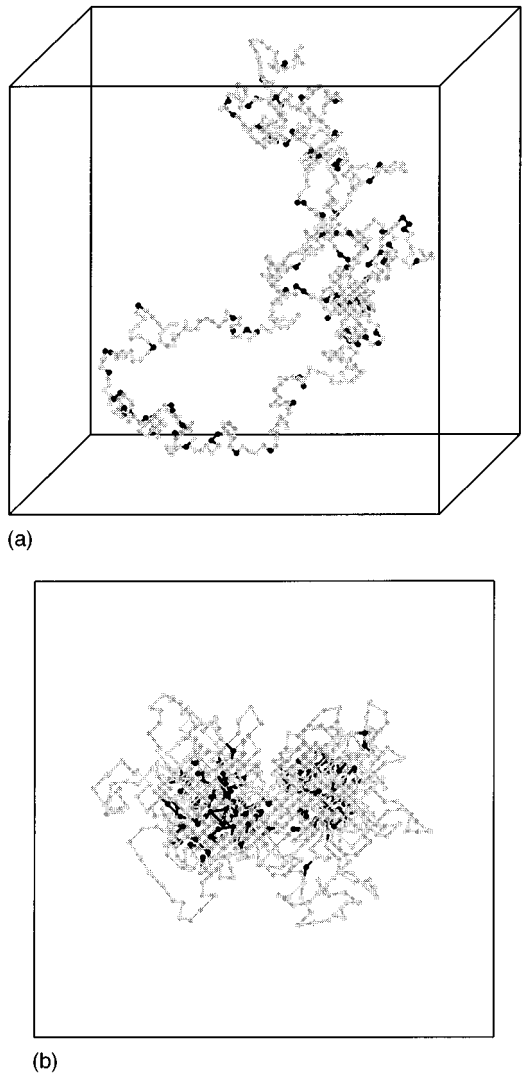

FIG. 12. Equilibrium copolymer configurations for degree of polymerization $N=768$ and hydrophobic bead concentration $n_a=1/8$ on the lattice $L=128$. Pictures (a) and (b) correspond respectively to the Flory coil state and ''collapsed'' state. Hydrophobic monomers are drawn in black and hydrophilic in grey. The frame size in (b) is equal to 32 lattice units.

marked (II) we see some sort of intermediate situation where the single micellelike structure often fluctuates and breaks up, and multiple micelle structures can join. We are unclear as to whether this is some crossover regime, or a genuine transition which has been softened because the chains are still relatively short.

We may also note that the radius of gyration of the ''collapsed'' state and, more importantly, its swelling exponent ν, appears to be dependent on the hydrophobic concentration n_a. Some particular values of the effective swelling exponents ν for different concentrations n_a are presented in Table IV. One can see that for concentrations in the range $1/5 \leqslant n_a \leqslant 1$ the collapse exponent is essentially unaffected, while for the smallest concentrations the values of ν_c^{eff} are close to the Flory exponent. As mentioned above, possibly one is merely seeing some crossover phenomenon. It remains possible however, that the ''collapsed'' phase is actually more than one type of state with different clearly defined

TABLE IV. Values of the effective swelling exponent ν_c^{eff} of the ''collapsed'' state versus the hydrophobic concentration, n_a obtained for the degrees of polymerization $N=60$, 120, 180, 240.

n_a	1/15	1/12	1/10	2/15	1/6	1/5	1/4	1/3	1/2
ν_c^{eff}	0.58	0.56	0.52	0.47	0.405	0.342	0.338	0.337	0.336

Flory exponents. It certainly seems reasonable to suppose that the chain of micelles state [region (III)] for large hydrophilic concentrations n_b is a renormalized Flory coil. In this case the ''collapse'' transition line must terminate in an end point of some sort. This is quite consistent with the first entry for $n_a=1/15$ in Table IV. It would be interesting to have some clear theoretical predictions for all of these phenomena. We view the hydrophobic screening of various core arrangements as a most important observation, and shall have more to say on that issue in the conclusion.

It is interesting to compare the result (22) with what one can expect from a naive mean-field model.[33] First, suppose that one can still approximate the model by a diagonal effective potential ΔV_q of the Fourier modes as in Ref. 10. Second, let us use the following additional condition $u_2^{ab}=(u_2^{aa}+u_2^{bb})/2$, that relates the second virial coefficients of monomer pairs of different types. Under these assumptions it is possible to rewrite the Gaussian self-consistent equation as one for a homopolymer with the effective second virial coefficient $u_2^{\text{eff}}=n_a u_2^{aa}+n_b u_2^{bb}$, which yields a rather rough mean-field law $\chi_c \simeq \chi_c^{(h)}/n_a$ rather than (22). Clearly this type of thinking is not appropriate.

The answer may lie in the following observation. Thus, for $n_a \gtrsim 1/5$ we determine the final state of the collapsed coil to be a single ''micellelike'' object in which the hydrophobic material is buried in the core, and hydrophilic units are largely located at the surface. This is illustrated in Fig. 12(b) and discussed a little later when we come to compare equilibrium and kinetic behavior, but for the present purpose we can say that this collapsed state may be viewed as having arisen from a macroscopic ''phase separation'' of hydrophobic and hydrophilic monomer units. We may ask, therefore, how the characteristic phase-separation energy scale $\chi_c(n_a)$ increases with increasing n_a. The only relevant scale seems to be that due to the interface between the hydrophobic core and hydrophilic shell, and is therefore a sort of interfacial energy. Therefore, assuming the interfacial area scales as $(R_g^0)^2$, where R_g^0 is the hydrophobic core radius, we may make the estimate,

$$\chi_c(n_a) \propto 1/(R_g^0)^2 \propto n_a^{-2/3}, \tag{23}$$

since for a collapsed core $R_g^0 \propto n_a^{1/3}$. These arguments break down as n_a becomes smaller since the equilibrium state is then no longer a single ''micelle–like'' object. The curve $\chi_c(n_a)$ in this regime no longer fits the law of equation (22), and as yet we have no arguments for its form.

Now, we turn to the nature of the transition itself. One possibility has been discussed recently.[28,33] Thus using the replica trick, and then ground state dominance without replica symmetry breaking, has been argued that the ''collapse'' transition may ultimately become first order for low hydro-

phobic compositions. However, though we do find metastable states in our simulation, a matter to which we shall presently turn, we have not been able to rationalize our results on the basic of a first order transition. Thus, as expected, the heat capacity plot in Fig. 2 for the homopolymer is consistent with a continuous transition. On the contrary, as we depart from the homopolymer limit the disorder-averaged heat capacity broadens and becomes smoothed, as might be expected. This is not consistent with a first-order transition. Undoubtedly, there are many potential pitfalls in such an argument and very considerable finite-size studies may have to be undertaken before the matter is resolved. We caution the reader also that the topological frustration induced by competing interactions on connected chains may result in nonequilibrium heat capacities that appear to be equilibrium ones.[34] Despite all these reservations we note that there is another possible interpretation of the transition in this region. Thus, it remains possible that one is witnessing a type of glass transition. Evidently a careful consideration by theory and simulations must be devoted to this issue.

In the current paper we consider also kinetics at the ''collapse'' transition of random copolymers with small values n_a, i.e., copolymers which have the most nontrivial equilibrium ''collapsed'' states. We see that the first kinetic stage appears to proceed in a qualitatively similar manner to that of a homopolymer system. In the picture in Fig. 13(a) we show a particular copolymer configuration with the degree of polymerization $N=768$ for 1000 MCS after the quench. The first stage may still be characterized by formation of globules, as for homopolymers. However the source of cluster formation now appears to be in accumulations of hydrophobic monomers. We believe that, as for the homopolymer, there is a sort of spinodal decomposition in the metric of the polymer. In this case however the analogy is really closer to spinodal decomposition of a binary mixture. In Figs. 14 and 15 we show the time evolution of the radius of gyration square R_g^2 and the average cluster number $\langle n \rangle$. Here the degree of polymerization is equal to $N=240$ and the values of the concentrations n_a are 1/5 and 1/15. The total time depicted in those figures corresponds approximately to 1/2 of the total collapse time of a comparable homopolymer. One can see that the process of cluster formation at the first stage is somewhat slower than for homopolymers and the cluster number after the first stage is smaller. The decrease of the radius of gyration squared ΔR_g^2 is less significant and appears to be close to a linear law.

The second kinetic stage for copolymers with low hydrophobic concentration appears to be quite different to that for homopolymers. It seems that we now have very long-lived metastable states with configurations consisting of few globules that have similar internal structure as in the ''collapsed'' copolymer equilibrium state, that is hydrophobic cores surrounded by amphiphilic b-monomer shells. Later on these states will further collapse into fewer hydrophobic cores, many finally becoming a single micellelike object. In the picture in Fig. 13(b) we show an example of what we believe to be metastable copolymer configuration some 1 000 000 MCS after the quench. This example corresponds to a quench from point C to D in the phase diagram, Fig. 11. It is

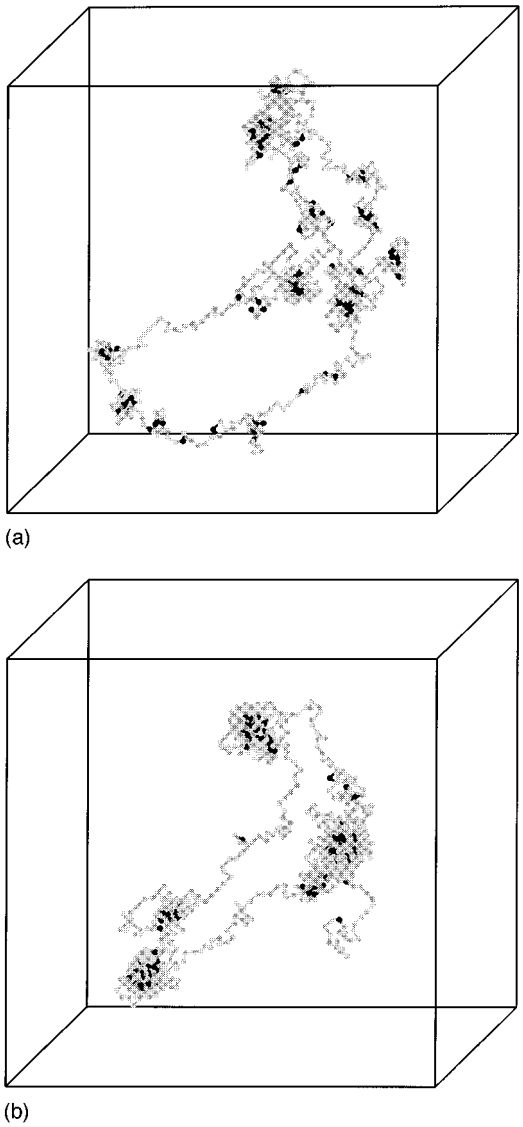

FIG. 13. Evolution of a particular copolymer configuration at the ''collapse transition'' for the degree of polymerization $N=768$ and hydrophobic bead concentration $n_a=1/8$ on the lattice $L=128$. Pictures (a) and (b) correspond respectively to times 1 000 and 1 000 000 MCS after the quench.

to be compared with the appropriate final equilibrium configuration of Fig. 12(b). Note that the metastable state is quite mobile.[35] However, the local amphiphilic shells deter unification of clusters and produce what seems to be a kinetic arrest in the binary mixture spinodal decomposition. This, then, is one of the key results of the kinetics studies. There exist quite extended polymer configurations which fluctuate substantially, and therefore have high entropy, but which are arrested far from equilibrium. We believe that in this picture one may find an understanding of some of the long-lived extended protein states that have long been a matter of debate in the bioscience community.[24,33]

VI. CONCLUSION AND DISCUSSIONS

Using the Monte Carlo lattice model of polymers we have studied kinetics at the collapse transition. Although this model does not possess independent modes, analysis of the

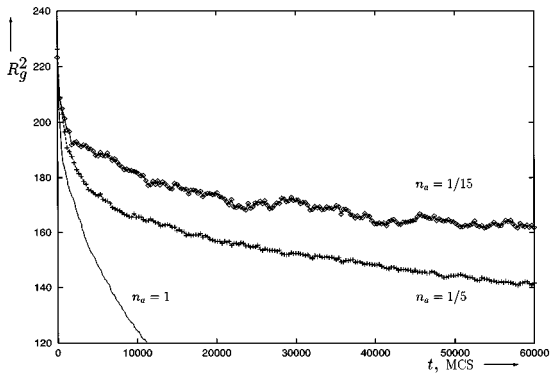

FIG. 14. The radius of gyration square R_g^2 during copolymer kinetics versus time for copolymers with the degree of polymerization $N=240$ for different hydrophobic bead concentrations n_a (from bottom to top): 1 (homopolymer), 1/5, 1/15. Equilibrium values of R_g^2 in the final state are: $R_g^2=19.3$ for $n_a=1/5$ and $R_g^2=73$ for $n_a=1/15$.

Fourier modes understood in the sense of a formal transformation of variables proves to be quite useful and of importance for the radius of gyration (8). First of all, we find good agreement with the prediction of the Gaussian self-consistent model[11] for the law $\Delta R_g^2 \propto t^{7/11}$ at small times. Also we can clearly see (Figs. 4, 6, and 10) the local clusters growth mechanism. Although this mechanism is radically different from that of the ''sausage model,''[17] we are still in agreement with total collapse time scaling $\tau \propto N^2$ in that model without hydrodynamics. In the framework of the Gaussian self-consistent model this law can be written as $\tau \propto N^{2\beta_{\rm eff}}$, where $\beta_{\rm eff}$ is the effective value of the time-dependent Flory exponent. Our interpretation is that this value can be approximately taken as $\beta(t)$, and changes in the range $5/6 \leqslant \beta(t) \leqslant 3/2$, during the middle collapse stage. One can see from Fig. 8 that we have $\beta_{\rm eff} \simeq 1$, which is the θ-point exponent, though from the Gaussian self-consistent theory[11] one would expect instead the lower bound value $\beta_c=5/6$ at the final stage of kinetics.

These conclusions are crucially different from that of the irreversible end-dominated collapse[4] $\tau \sim N$. This is hardly surprising taking into account the differences between the models. First, hydrodynamics effects are not accounted for in our approach. This is more tractable in a continuous space Langevin calculations with the Oseen tensor and work is continuing in this direction.[36] The method employed in Ref. 4 corresponds to an effective accounting for hydrodynamics since the authors allow moves of sufficiently big clusters as a whole according to Stokes law $D \sim N^{-1/3}$. Also, units are absorbed irreversibly onto clusters. Naturally in such a scheme the end clusters are more mobile and grow faster. In our simulations with moderate quenches, clusters are not quite dense objects, their boundary is quite labile and able to dissociate. We have checked to see if, in our case, the end clusters move more rapidly, and found that such a conclusion is not justified.

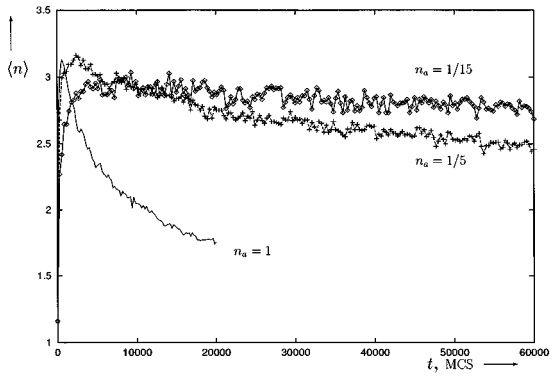

FIG. 15. The average number of clusters (during copolymer collapse kinetics) $\langle n \rangle$ versus time for copolymers with degree of polymerization $N=240$ for different hydrophobic bead concentrations n_a (from bottom to top): 1 (homopolymer), 1/5, 1/15.

The results for the copolymers are somewhat more unusual. The equilibrium phase diagram is beginning to become clear. The homopolymer collapse transition extends to become a curve in the composition of the copolymer. At low hydrophilic content the collapsed phase possesses a hydrophobic core with hydrophilic exterior. This is analogous to a macroscopic phase separation of the two different components. As the amount of hydrophilic component increases we find that the single micelle breaks into a self-avoiding chain of micelles, with the collapse transition curve, possibly, terminating in an end point, so that the Flory phase is continuously connected to the ''collapsed'' phase. The collapse transition for a homopolymer is continuous, but for the copolymer we have reason to believe that a type of glass transition occurs. We find no evidence of a discontinuous transition, though we agree that is might be expected on the basis of earlier theoretical calculations.[28]

Finally, the ''collapse'' kinetics across this portion of the transition is quite distinctive. This is illustrated by reviewing Fig. 12 representing initial and final states, and Fig. 13(b) representing a very long-lived kinetic state in between. The initial stage of collapse, shown in Fig. 13(a), is rather like spinodal decomposition of a binary fluid, but in the metric of the chain, rather than by analogy with our conclusion for the homopolymer. Later on, relaxation across the transition is very slow, and there appear to be numerous quite stable intermediate states in which small ''micellelike'' objects form along the chain with hydrophilic group screening the hydrophobic material from further collapse. Again, one might suspect a kinetic arrest has occurred, rather what one would expect in the vicinity of a glass transition. The kinetic laws in this regime are not yet known, but one can conjecture that something akin to glass relaxation occurs.

Perhaps we can make a few practical experimental points too. It is known that for homopolymers in water solution at reasonable concentrations it is essentially impossible to separate collapse from aggregation.[31] From our discussion of copolymers we can predict that at modest hydrophilic concentrations, careful experiments may be able to see collapse isolated from aggregation because of the hydrophilic screening. In addition, besides the natural spectroscopic studies, direct evidence for these phenomena may come from selective deuterium labeling of the hydrophilic and hydrophobic monomer species, before polymerization. This would permit

contrast small angle neutron scattering studies to prove the concepts discussed here.

In conclusion, the situation with respect to homopolymers is relatively clear despite a few remaining puzzles. Unfortunately, the copolymer case is far from solved, and considerable efforts both by theory and simulations will yet be required to do so. However, based on our work it seems likely that the necessary simulations are possible. For the moment the status of the equilibrium theory is still uncertain, and theory of the kinetics has not yet been presented. It will be of importance to make progress here since, if there is a deeper story to be told for the case of protein folding kinetics, there is every likehood that this story will unfold in the context of the current problem.

ACKNOWLEDGMENTS

The authors acknowledge interesting discussions with Professors P. G. de Gennes, A. R. Khokhlov, P. Pincus, Y. Rabin, and Dr. A. Gorelov. This work was supported by DEC and the Irish Government.

[1] M. Doi and S. F. Edwards, *The Theory of Polymer Dynamics* (Oxford Science, New York, 1989).
[2] P. G. de Gennes, *Scaling Concepts in Polymer Physics* (Cornell U.P., Ithaca, NY, 1988), 3rd printing.
[3] J. des Cloizeaux and G. Jannink, *Polymers in Solution* (Clarendon, Oxford, 1990).
[4] B. Ostrovsky and Y. Bar-Yam, Comp. Polym. Sci. **3**, 9 (1993).
[5] A. Byrne, P. Kiernan, D. Green, and K. A. Dawson, J. Chem. Phys. **102**, 573 (1995).
[6] *Monte Carlo Methods in Statistical Physics*, edited by K. Binder (Springer-Verlag, Berlin, 1986), 2nd ed.; *Applications of Monte Carlo Method in Statistical Physics*, edited by K. Binder (Springer-Verlag, Berlin, 1987), 2nd ed.; M. P. Allen and D. J. Tildesley, *Computer Simulations of Liquids* (Clarendon, Oxford, 1987); H. P. Witmann and K. Kremer, Comput. Phys. Commun. **61**, 309 (1990); M. A. Smith, Y. Bar-Yam, Y. Rabin, B. Ostrovski, C. A. Bennett, N. Margolus, and T. Toffoli, Computat. Polym. Sci. **2**, 165 (1992).
[7] D. J. Flory, *Statistical Mechanics of Chain Molecules* (Wiley, New York 1979).
[8] M. A. Smith, Y. Bar-Yam, B. Ostrovsky, Y. Rabin, C. H. Bennett, and T. Toffoli, J. Comp. Pol. Sci. **2**, 165 (1992); Y. Bar-Yam, Y. Rabin, and M. A. Smith, Macromol. Reprints **25**, 2985 (1992).
[9] In practice, we increase the lattice in each direction by the number of cells equal to the interaction range and forbid monomers to occupy those positions.
[10] E. G. Timoshenko and K. A. Dawson, Phys. Rev. **E 51**, 492 (1995).
[11] E. G. Timoshenko, Yu. A. Kuznetsov, and K. A. Dawson, J. Chem. Phys. **102**, 1816 (1995).
[12] By mean-field we mean, of course, Flory theory. In some sense there has never been a true mean field theory of polymer, according to the normal standards of statistical mechanics.
[13] Roughly speaking, we expect the equilibration time to scale $\tau \sim N^2$. Therefore, we always equilibrate each sample for a small multiple of this fundamental relaxation time, until the averages are stable. The collapsed averages are obtained by slow annealing, with this relaxation procedure being applied at each step. A number of separate anneals are made until the final averages are stable. We note that the results in Table I are therefore obtained from many millions of MCSs, considerably more that those of Fig. 9.
[14] E. G. Timoshenko, Yu. A. Kuznetsov, and K. A. Dawson, Phys. Rev. E (submitted).
[15] K. A. Dawson, E. G. Timoshenko, and P. Kiernan, Proceedings of the First International Conference on ''Scaling Concepts and Complex Fluids,'' Catanzaro, 4–8 July, 1994, in Nuovo Cimento **16D**(7) (1994); K. A. Dawson, E. G. Timoshenko, and P. Kiernan (unpublished).
[16] D. Bratko and K. A. Dawson, J. Chem. Phys. **99**, 5352 (1993).
[17] P. G. de Gennes, J. Phys. Lett. **46**, L639 (1985).
[18] At this point we note, though we have suppressed details, considerable effort has been extended to establish results with good statistical accuracy. In some cases the errors are given explicitly. In others the accuracy is implied by the precision of the result. We note that the status of the present results is, in these respects, quite different from an earlier work (Ref. 5) of ours, where the complexity of the model did not permit such rigor.
[19] We caution the reader that, though we are confident of the exponent, we can argue for more than one origin of the result. For example, ''local mobility'' arguments may also give $\alpha = 3/5$. We believe that we have a theory for $\alpha = 7/11$, however, as Eq. (14) discussed above.
[20] By sufficiently large q we mean large compared to the characteristic unstable mode, but smaller than the microscopic cutoff or lattice spacing.
[21] E. M. Lifshitz and L. P. Pitaevskii, *Physical Kinetics* (Pergamon, New York, 1981), p. 427.
[22] We note, from Table III that considerable care must be taken to obtain the coarsening exponent Z_N since it is only at the longest chain length that we find limiting behavior. Thus, extrapolation in N is necessary, and one should doubt estimates that preclude this possibility.
[23] A. Grosberg and S. Nechaev, J. Phys. A: Math. Gen. **25** 4659 (1992); A. Yu. Grosberg and D. V. Kuznetsov, Macromolecules **26**, 4249 (1993); E. Shakhnovich and A. Gutin, Nature (London) **346**, 773 (1990).
[24] H. A. Scheraga, Pure Appl. Chem. **36**, 1 (1973); N. Go and H. Taketomi, Proc. Natl. Acad. Sci. USA **75**, 559 (1978); O. Ptitsyn and A. Finkelstein, Q. Rev. Biophys. **13**, 339 (1980); P. Privalov, Adv. Protein Chem. **35**, 1 (1982); J. Bryngelson and P. Wolynes, Proc. Natl. Acad. Sci. USA **84**, 7524 (1987); O. Ptitsyn, J. Protein Chem. **6**, 273 (1987) T. Garel and H. Orland, Europhys. Lett. **6**, 307 (1988); H. Frauenfelder, F. Parak, and R. Young, Annu. Rev. Biophys. Biophys. Chem. **17**, 451 (1988); E. Shakhnovich and A. Gutin, Nature (London) **346**, 773 (1990); E. Shakhnovich, G. Farztdinov, A. M. Gutin, and M. Karplus, Phys. Rev. Lett. **67**, 1665 (1991); M. Matsumoto *et al.*, J. Polym. Science B **30**, 779 (1992); *Protein Folding*, edited by T. E. Creighton (Freeman, New York, 1992); K. Minagawa, Y. Matsuzawa, Y. Yoshikawa, A. R. Khokhlov, and M. Doi, Biopolymers **34**, 555 (1994); *New Developments in Theoretical Studies of Proteins*, edited by R. Elber (World Scientific, Singapore, 1994).
[25] A. Yu. Grosberg and D. V. Kuznetsov, Macromolecules **26**, 4249 (1993); A. Yu. Grosberg, Y. Rabin, S. Havlin, and A. Nir, Europhys. Lett. **23**, 373 (1993); V. S. Pande, A. Yu. Grosberg, and T. Tanaka, J. Chem. Phys. **101**, 8246 (1994).
[26] C. Tanford, *The Hydrophobic Effect* (Wiley, New York, 1980); K. A. Dill, Biochemistry **29**, 7133 (1990).
[27] S. P. Obukhov, J. Phys. A, **19**, 3655 (1986).
[28] T. Garel, L. Leibler, and H. Orland, Preprint SPhT/94–077, Saclay.
[29] J. D. Honeycutt and D. Thirumalai, Biopolymers, **32**, 695 (1992); P. E. Leopold, M. Montal, and J. Onuchic, Proc. Natl. Acad. Sci. USA, **89**, 9721 (1992); C. J. Camacho and D. Thirumalai, Phys. Rev. Lett. **71**, 15, 2505 (1993).
[30] C. D. Sfatos, A. M. Gutin, and E. I. Shakhnovich, Phys. Rev. E **50**, 2898 (1994); A. M. Gutin and E. I. Shakhnovich, *ibid.* **50**, R3322 (1994).
[31] Y. Chang, Y. Lochhead, and C. L. McCormick, Macromolecules **27**, 2145 (1994); A. Gorelov and K. A. Dawson (unpublished); A. du Chesne, A. Gorelov, and K. A. Dawson (unpublished).
[32] C. D. Sfatos, A. M. Gutin, and E. I. Shakhnovich, Phys. Rev. E **48**, 465 (1993).
[33] Yu. Kuznetsov and K. A. Dawson (unpublished); A. Moskalenko and K. A. Dawson (unpublished).
[34] K. A. Dawson, B. L. Walker, and A. Berera, Physica A, **165** 320 (1990).
[35] It can be seen from Figs. 14 and 15 that data for small concentrations n_a are more noisy despite the fact that data for all hydrophobic concentrations were obtained from the same ensemble set.
[36] A. Byrne, P. Kiernan, and K. A. Dawson (unpublished).